Investigation of the Effects of Rotor Pole Geometry and Permanent Magnet to Line Start Permanent Magnet Synchronous Motor's Efficiency

İlhan Tarımer

Department of Electronics and Computer Education, Technical Education Faculty, Muğla University
Kötekli Campus, 48000, Muğla, Turkey, phone: +90 252 211 1722, e-mail: itarimer@mu.edu.tr

Introduction

For three decades a number of authors have investigated the usage of LSPMSM motors as a replacement for induction motors. As long ago as 1978, Binns [1] produced a review of the development of self starting synchronous motors. At that time, they concluded that it was probably necessary to use finite-element techniques to accurately predict the performance of LSPMSM motors. In the two decades since that work was published, interest in these motors has been sporadic. In 1980, Honsinger [2, 3] used generalized machine equations in an attempt to describe the performance of these motors when operating under either synchronous or dynamic conditions. Since then efforts have been made to simulate steady-state performance using finite-element techniques. Some of these papers, such as those by Binns [4] and Shimmin [5], applied finite-element models to provide parameters for circuit models, while others, such as Kurihara [6] and Williamson and Knight [7] applied time-stepping finite-element models.

In this paper, the author has used Rmxprt software in order to simulate LSPMSM machines and made analytical analysis of them. These simulations and calculations have given comparison occasion amongst LSPMSM machines having different rotor types. The LSPMSM motors are capable of not only the direct operation of the commercial voltage source but also high efficiency improvement than the efficiency of IMs in steady state. In addition, it is possible to achieve unity-power-factor performance, with reduced stator currents and corresponding losses [8–11]. A good design for an LSPMSM motor has to fulfill three main requirements. It must provide sufficient asynchronous torque across the full speed range during starting. In addition, it must use as little permanent-magnet material as possible to keep material costs low, but still provide sufficient excitation to allow near-unity power factor synchronous operation at full load [12–14].

Here, efficiencies of LSPMSM having several rotor geometries have been examined. To achieve this aim, 550 Watts LSMPSMs which have eight type rotors have been simulated. So, several electrical parameters like efficiency, $\cos\varphi$, magnetic flux density, starting torque have been obtained in better values for T5.

Understanding of LSPMSM from Aspect of Electrical Parameters

Synchronous motors use three-phase sinusoidal voltage source to induce a rotating magnetic field inside stator. Applying this three-phase sinusoidal voltage source to the stator winding of a synchronous motor yields the rotational magnetic field in the air gap. The permanent magnet poles mounted on the rotor try to align in this rotating field, producing a synchronous torque on the rotor. Upon starting, the damping winding on the rotor generates the asynchronous starting torque, creating a self-starting feature [15, 16]. The phasor diagram for the line-start permanent-magnet synchronous motor (LSPMSM) in the frequency domain is shown in Fig. 1.
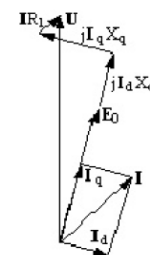

Fig. 1. Phasor diagram of LSPMSM

In Fig. 1, R_1, X_d, and X_q are armature resistance, d-axis synchronous reactance, and q-axis synchronous reactance, respectively. X_d is the sum of leakage reactance, X_1 and d-axis armature reactance X_{ad}, and X_q is the sum of X_1 and q-axis armature reactance X_{aq}. For a given torque angle θ, the angle that $\mathbf{E}_0$ lags $\mathbf{U}$, the followings can be obtained (1):

$$I_d * X_d + I_q * R_1 = U * I_d * R_1 + I_q * X_q = U * \sin\theta . \quad (1)$$

I_d and I_q can then be derived from the following two equations (2), (3):

$$I_d = (X_q * (U * \cos\theta_0 - E_0) - \frac{R_1 * U * \sin\theta}{R_1 * R_1 + X_d * X_q} ; \quad (2)$$

$$I_q = (R_1 * (U * \cos\theta_0 - E_0) - \frac{X_d * U * \sin\theta}{R_1 * R_1 + X_d * X_q} . \quad (3)$$

The angle that **I** lag **E**$_0$ is found using (4):

$$\psi = \text{tg}^{-1}(\frac{I_d}{I_q}) . \quad (4)$$

The power factor angle (or torque angle) that **I** lags **U**, is found using (5):

$$\varphi = \theta + \psi . \quad (5)$$

The input power (electric power) can now be computed from voltage and current as:

$$P_1 = 3 \cdot U \cdot I \cdot \cos\varphi . \quad (6)$$

The output power (mechanical power) is:

$$P_2 = P_1 - (P_{fw} + P_{cu} + P_{Fe}) , \quad (7)$$

where P_{fw}, P_{Cu}, and P_{Fe} are frictional and wind loss, armature copper, and iron-core loss, respectively. The output mechanical power (torque) T_2 is:

$$T_2 = \frac{P_2}{\omega} , \quad (8)$$

where ω is the synchronous speed in rad/s.

The efficiency is computed by following expression:

$$\eta = \frac{P_2}{P_1} 100\% . \quad (9)$$

The motor is started to operate in the same way as for an induction motor, by using a squirrel-cage-type winding, called a damper winding in this case, that is mounted on the rotor, producing the starting torque.

Geometrical Shapes of Rotor Pole Types

Some of these rotor pole types are not suitable for required high efficient system. In recent years, industrial applications have become to need more high efficient system. In this paper, the author has researched to define if all other motor parameters is as the same, which model type better and has high efficient. The rotor types investigated have been demonstrated in Fig. 2–3.
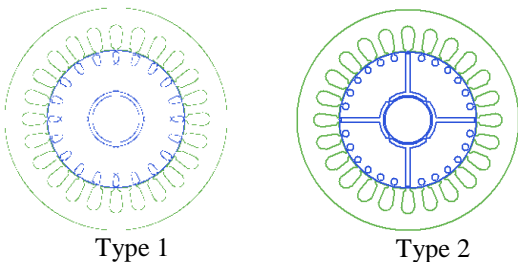

Type 1   Type 2
Fig. 2. The rotor types which inspected [1]

RMxprt Analysis of LSPMSM

In this section, application of finite element analysis (FEA) has been used for the magnetic field computation. As paralel to this, analysis of performance of LSPMSM machine with different rotor configurations has been presented. As known, FEA is a useful tool for improving the existing design of LSPMSM machines towards the performance improvement and design optimization of these machines. Ansoft Rmxprt software is used for calculating the transient and steady state parameters of motor. To do this, the following field equation in matrix form can be used as in (10):

$$[S]\{A\} + [T]\frac{d}{dt}\{A\} + [H]\{i_f\} + [D]\{V_b\} + [E]\{i_s\} = \{g\}, \quad (10)$$

where A – magnetic vector potential at the nodes of the mesh; if – terminal current vector flowing into each winding; V_b – unknown vector of induced voltage; I_s – the source component; g – the excitation vector.

Type 3   Type 4

Type 5   Type 6
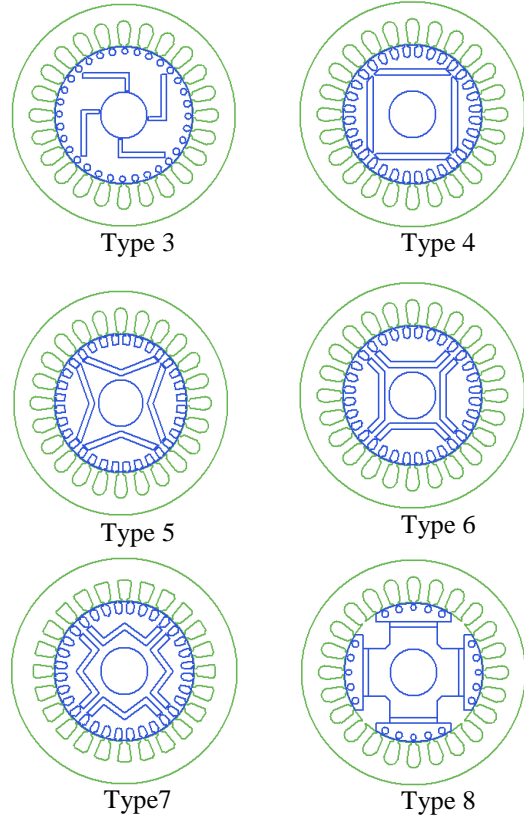
Type7   Type 8

Fig. 3. The rotor types which inspected [2]

The rotor structures shown in Fig. 2–3 are known and called as T1, T2 (radially magnetized rotor), T3 (asymmetrically distributed rotor), T4, T8 (embedded magnet rotor), T5 (inset magnet rotor) and T6, T7 (interior magnet rotor).

For stranded windings (11) and (12) can be written as:

$$[H]^T\frac{d}{dt}\{A\} + [R]\{i_f\} + [L]\frac{d}{dt}\{i_f\} + [\Gamma]\{u_c\} = \{u_s\} , \quad (11)$$

$$[\Gamma]^T\{i_f\} + [C]\frac{d}{dt}\{u_c\} = \{0\} . \quad (12)$$

For squirrel cage type of motors, rotor bars are connected by end rings. By taking squirrel cage as a polyphase circuit, the following circuit equation is used to account for the end effects.

$$[D]^T \frac{d}{dt}\{A\} + [B]\{V_b\} = \{q\} . \qquad (13)$$

"B" is derived from the resistance and the inductance of end ring. The source compenent $\{i_t\}$ to be solved in solid conductors as in (14):

$$[E]^T \frac{d}{dt}\{A\} + [N]\{i_S\} = \{i_t\}. \qquad (14)$$

The resultant system equations can be summarized in matrix form as :

$$[M_{nn}]\{X_n\} = \{y_n\}, \qquad (15)$$

where index **n** denotes total number of unknowns and can be described as motion of the rotor expressed in (16):

$$J\alpha + \lambda\omega = T_{em} + T_{app} ; \qquad (16)$$

where ω – angular velocity; α – angular acceleration; J – moment of initeria; λ – damping coefficient; T_{em} – electromagnetic torque; T_{app} – applied mechanical torque.

Fig. 4 demonstrates two different simulations of motor phase current and efficiency versus rotor types.
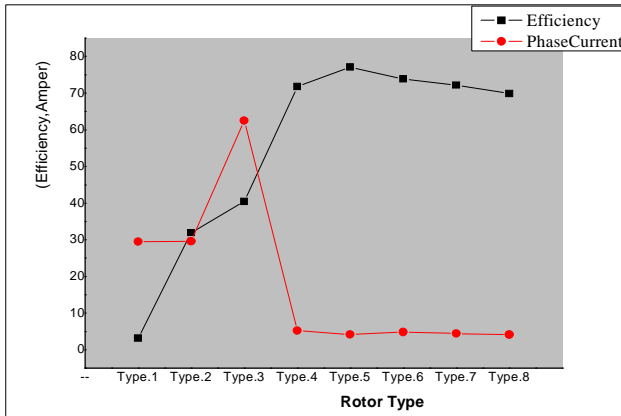

Fig. 4. Simulation of motor phase current and efficiency versus rotor types

As shown in Fig. 4, phase currents would flow as high in rotor types T1, T2 and T3 but these motors would deliver low efficiency. T4, T5, T6, T7, and T8 have similar phase current/efficiency value. Amongs these rotor types, T5 has better efficiency and lower phase current values than other rotor types. The stator of LSPMSM is very similar to that of a polyphase induction motor. In last decade,researchers have been studied on various geometries of LSPMSM. They were usually based on the further improvements of power density and efficiency by adopting flux enhancement, armature reaction and reduction. But changing of rotor types can directly have a relationship of LSPMSM efficiency.

Efficiency and $\cos\psi$ variation according to rotor types have been presented in Fig.5. They were produced by using a coarse mesh.
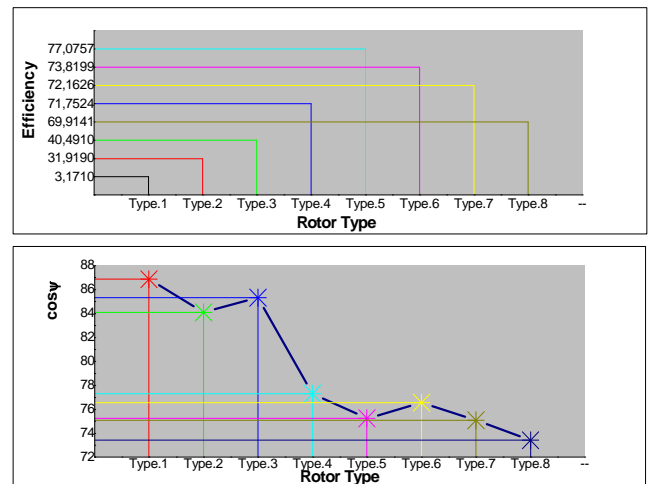

Fig. 5. Variations of efficiency and $\cos\psi$ versus rotor types

However the types T4, T5, T6, T7 and T8 presented in Fig.5 are suitable for practical applications , the types T1, T2 and T3 are pratically out of commercial using, because of having low efficiency values. The characteristics of magnetic flux density versus rotor types can be seen from Fig. 6.
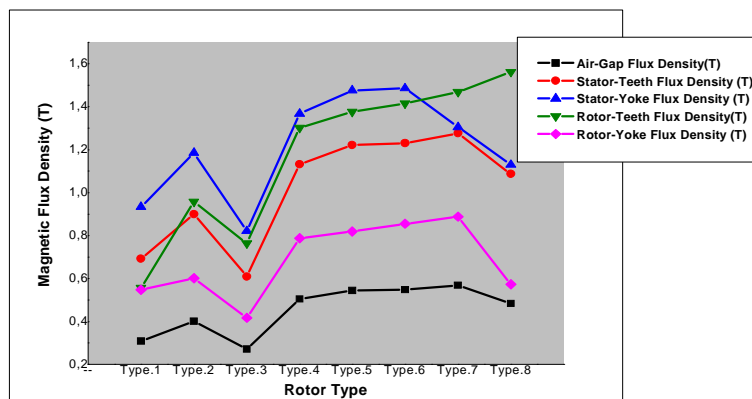

Fig. 6. Simulations of stator and rotor teeth, yoke and air-gap flux densities versus rotor types
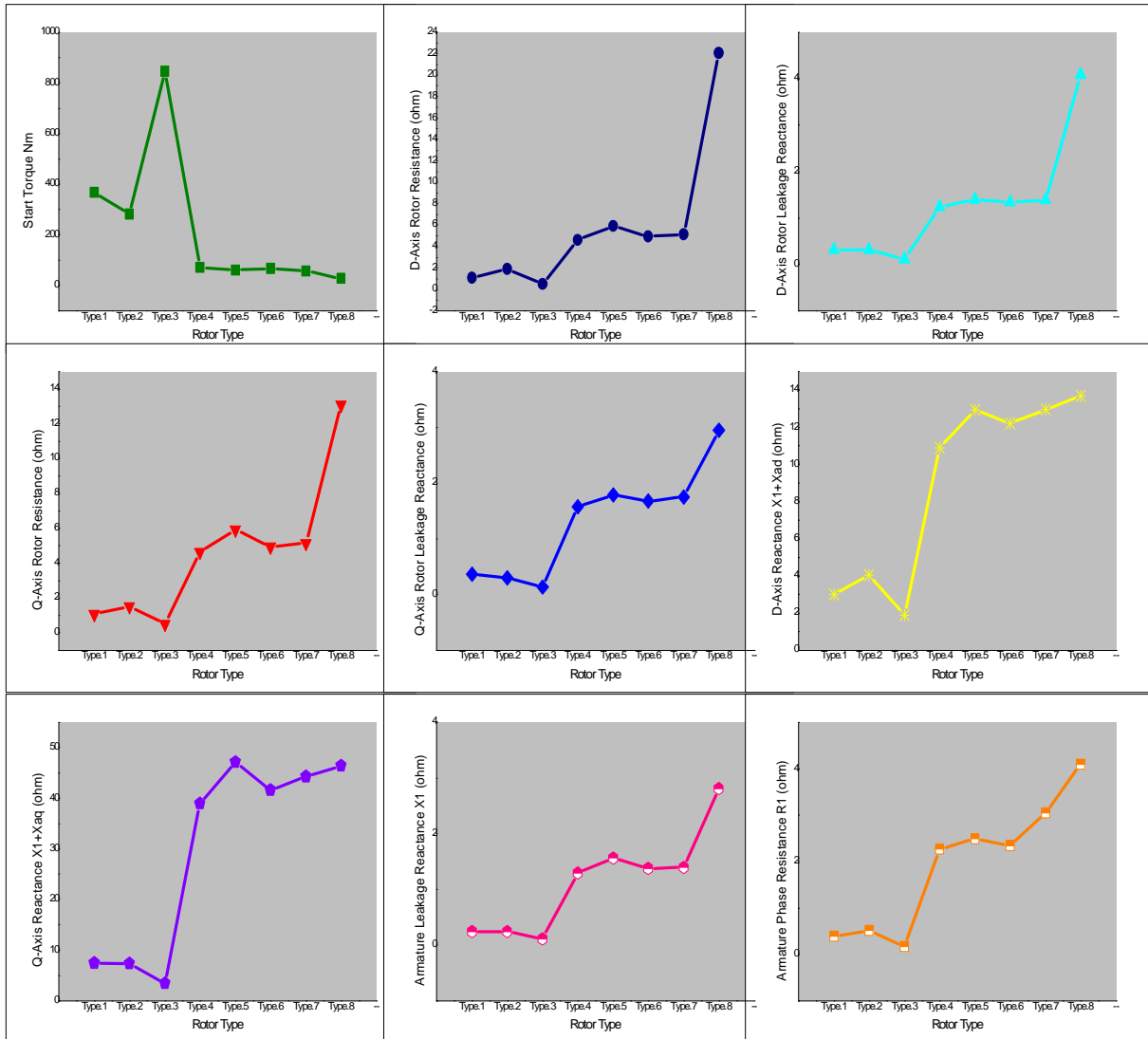
Fig.7. Simulations of steady state and transient parameters versus different rotor types

The start-up transients of LSPMSM synchronous motors presents similar characteristics to standard IMs during such a transient. In fact, the rotor cage develops an asynchronous torque similar to that produced in an induction machine, that only works when PM synchronous motor is not synchronized or when the load angle ψ changes. Steady state and transient parameters have been calculated and simulated for different parameters have been calculated and simulated for different rotor types and presented in Fig. 7.

As known, because of LSPMSMs have got damper windings, they produce asynchronous torque during their starting. From the first graphics in Fig. 7, it is seen that the 3rd rotor type's starting torque will be the highest. As to be understood, the best suitable choice would be type 3 (T3). Amongst the second, third and fourth graphics in Fig.7, type 8's rotor configuration has bigger D-axis rotor resistance rather than the other types. Type 8 LSPMSM engenders bigger torque. From the other graphics in Fig.7, D and Q axis reactances of types 4, 5, and 7 have been obtained as closer to each others. Because, the structures of the type 4, 5, 6 and 7 seem similar to each others. The

cases of armature leakage reactance versus rotor types have been demonstrated at the last graphics in Fig.7. The rotor structures of types 1, 2, 3 and types 4, 5, 6, 7 seem similar to each others. So, there wouldn't occur conspicuously disparity amongst themselves. But, at the transitions from graphic 3 to 4 and graphic 7 to 8, salient augmentations on armature leakage reactance can be seen. Increasing of stator and rotor resistance has been caused more loss than motors have same parameters. The last graphics in Fig.6 shows relationship between rotor types and phase resistances. From this graphic, there is a distinctive difference on augmentation of phase resistances for solely rotor types 7 and 8. Because, particularly the structure of magnet in rotor type 7 is closer to rotor slots.

The graphics of rotor types versus output power and efficiency are given in Fig.8 and the graphics of motor $\cos\psi$ variations versus output power are given in Fig.9. Because of the rotor structures of type from 4 to 7 are similar; values of output power and efficiency have been closer to each others. The rotor structure of type 5 has the highest efficiency amongst these motors. However the motor which has the structure as type 1 will deliver the

biggest power factor, the efficiency of this structure is the least. In this case, it can be said that types from 4 to 8 would give similar characteristics of power factor versus output power to each others.

In this study while doing all simulations, LSPMSMs which have XG196/96 numbered magnets inside their rotor

geometries have been investigated. Beyond this, the effects of using different magnets according to different design requirements to motor efficiency have also been listed in Table 1. In this table, the effects of rotor structure and permanent magnet to motor efficiency have been indicated.
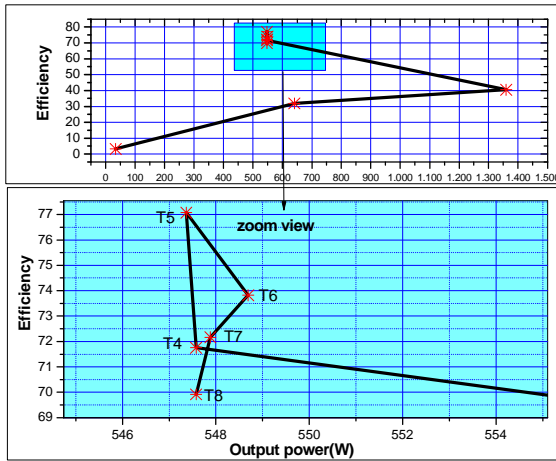

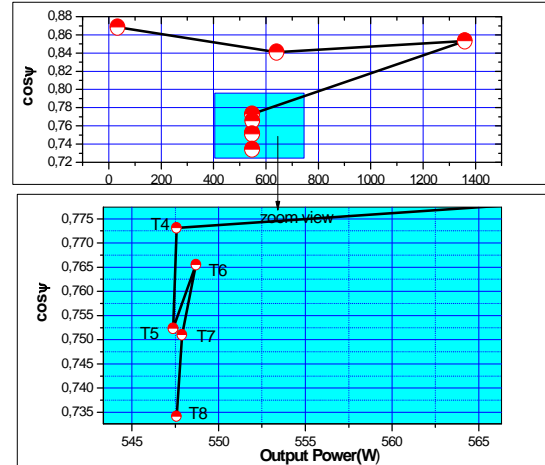**Fig. 8.** Efficiency and output power variation of rotor type

Fig. 9. Cosψ and output power variation of rotor type

Table 1. Simulated motor efficiency variation of permanent magnet with rotor type

P.Magnet	Type.1 η = Efficiency	Type.2 η = Efficiency	Type.3 η = Efficiency	Type.4 η = Efficiency	Type.5 η = Efficiency	Type.6 η = Efficiency	Type.7 η = Efficiency	Type.8 η = Efficiency
Alnico9	%34.833	%27.234	%16.7253	%71.8088	%75.7019	%71.9312	%70.3599	%72.1448
SmCo28	%48.625	%38.08	%26.258	%75.505	%80.0608	%77.3313	%76.1651	%73.8779
NdFe35	%38.8872	%32.9771	%29.9947	%78.7644	%81.5273	%78.9157	%76.9568	%76.692
XG196/ 96	%3,1710	%31,919	%40,4910	%71,7524	%77,0757	%73,8199	%72,1626	%69,9141

At the end of the simulations done with different magnets, for four genus magnets, eight types of rotor structure have been investigated. The maximum efficiency has been obtained from the motor (T5) in which NdFe35 were used.

Conclusions

In this paper, effect of rotor pole geometry to line start permanent magnet synchronous motor's efficiency has been presented. Inset magnet and interior magnet rotor types provide higher efficiency. Changing of permanent magnets raises motor's efficiency and get better. NdFe35 provide maximum permanent flux density on surface of rotor. Finally it has been seen that the rotor type (T5) and magnet's material type NdFe35 would provide high efficiency and power density in LSPMSM. It must be noticed that various machine parameters and designs contained different running conditions are important factors which affect efficiency too. Because of the fact that in high running temperature, it can be proposed to use SmCo28 instead of using NdFe35.

References

1. **Binns K. J., Barnard W. R. and Jabbar M. A.** Hybrid Permanent–magnet Synchronous Motors // Proc. Inst. Elect. Eng. – Mar. 1978. – Vol. 125, No.3. – P. 203–208.
2. **Honsinger V. B**. Permanent Magnet Machines: Asynchronous Operation // IEEE Trans. Power App. Syst. – July1980. – Vol. PAS-99. – P. 1503–1509.
3. **Honsinger, V. B.** Performance of Polyphase Permanent Magnet Machines // IEEE Trans. Power App. Syst. – July 1980. – Vol. PAS-99. – P. 1510–1518.
4. **Binns K. J. and Jabbar M. A.** High field Self-starting Permanent Magnet Synchronous Motor // Proc. Inst. Elect. Engineering. – May 1981. – Vol. 128, No. 2. – P. 157–160.
5. **Shimmin D. W., Wang J., Bennett N. and Binns K. J.** Modeling and Stability Analysis of a Permanent-magnet Synchronous Machine Taking into Account the Effect of Cage Bars // Proc. IEEE Elect. Power Applications. – Mar. 1995. – Vol. 142, No. 2. – P. 137–144.
6. **Kurihara K., Wakui G. and Kubota T.** Steady-state Performance Analysis of Permanent Magnet Synchronous Motors Including Space Harmonics // IEEE Trans. Magnetics. – May 1994. – Vol. 30. – P. 1306–1315.
7. **Williamson S. and Knight A. M.** Performance of Skewed Single Phase Line-start Permanent Magnet Motors // IEEE

Trans. Industry Applications. – May/June 1999. – Vol. 35. – P. 577–582.

8. **Miller T. J. E.** Single-phase Permanent Magnet Motor Analysis // IEEE Trans. Industry Applications. – 1985. – No. 4. – P. 651–658.

9. **Rahman M. A. and Zhou P.** Analysis of Brushless Permanent Magnet Synchronous Motors // IEEE Trans. Industrial Electron. – Apr 1996. – Vol. 43, No. 2. – P. 256–267.

10. **Lovatt H. C. and Watterson P. A.** Energy stored in Permanent Magnets // IEEE Trans. Magnetics. – Jan. 1999. – Vol. 35, No.1. – P. 505–507.

11. **Knight A. M. and McClay C. I.** The Design of High-Efficiency Line Start Motors // IEEE Trans. Industry Applications. – November/ December 2000. – Vol. 36, No. 6. – P. 1555–1561.

12. **Zhou P., Stanton S. and Cendes Z. J.** Dynamic Modeling of Three Phase and Single Phase Induction Motors // Proceedings of IEEE International Electric Machines and Drives Conference. – Seattle, May 1999. – P. 556–558.

13. **Singh B., Singh B. P. and Dwivedi S.** A State of Art on Different Configurations of Permanent Magnet Brushless Machines // IE(I) Journal-EL. – June 2006. – Vol. 87. – P. 63–73.

14. **Ansoft** Maxwell 11.1 Help Guide for Rmxprt, Analysis Approach for Line-Start PM Synchronous Motors. – P. 1.

15. **Stoia D., Ilea D., Cernat M., Dezsi Al. B. and Jimoh A.** Stability of the Line-Start Permanent Magnet Synchronous Motor Sensorless Drive // IEEE. – March 5, 2007. – P. 1–4.

16. **Popescu M., Miller T. J. E., McGilp M. I., Strappazzon G., Trivillin N. and Santarossa R.** Line-Start Permanent-Magnet Motor: Single-Phase Starting Performance Analysis // IEEE Transactions on Industry Appl. – July/August 2003. – Vol. 39, No. 4. – P. 1021–1030.

İ. Tarımer. Investigation of the Effects of Rotor Pole Geometry and Permanent Magnet to Line Start Permanent Magnet Synchronous Motor's Efficiency // Electronics and Electrical Engineering. – Kaunas: Technologija, 2009. – No. 2(90). – P. 67–72.

The effects of rotor pole geometry to line start permanent magnet synchronous motor's efficiency are discussed. To achieve this goal, several LSPMSMs which have eight type rotors and 550 Watts power have been simulated and analyzed. It has inferred that inset magnet and interior magnet rotor types provided higher efficiency and maximum permanent flux density on surface of rotor. Changing of permanent magnets' material to NdFe35 raises motor's efficiency. As result, the use of inset magnet and interior magnet rotor types and magnet's material NdFe35 in LSPMSMs provide high efficiency and power density. It is suggested that SmCo28 material must be used on permanent magnet's surfaces in high operating temperatures for powerful LSPMSMs. Ill. 9, bibl. 16 (in English; summaries in English, Russian and Lithuanian).

И. Таример. Исследование эффективности геометрии полюсов двигателя // Электроника и электротехника. – Каунас: Технология, 2009. – № 2(90). – С. 67–72.

Рассматривается влияние геометрии полюсов ротора на еффективность двигателя линейного запуска с постоянным магнитом. Для этого проанализировано и смоделировано несколько восмиполюсных 550-ватных двигателей. Предполагается, что внутренний магнит и тип ротора позволяют достигнуть более высокую эффективность и максимальную плотность постоянного потока на поверхности ротора. Поменяв материал постоянного магнита на NdFe35, увеличилась эффективность двигателя и плотность мощности. Предлагается поверхности постоянных магнитов мощных двигателейб работающих при высоких температурах, покрывать материалом SmCo28. Ил. 9, библ. 16 (на английском языке; рефераты на английском, русском и литовском яз.).

İ. Tarımer. Rotoriaus poliaus geometrijos ir nuolatinio magneto įtaka linijinio paleidimo variklio efektyvumui // Elektronika ir elektrotechnika. – Kaunas: Technologija, 2009. – Nr. 2(90). – P. 67–72.

Aptariama rotoriaus polių geometrijos įtaka linijinio paleidimo nuolatinio magneto sinchroninio variklio (LSPMSM) efektyvumui. Šiuo tikslu išanalizuoti ir sumodeliuoti keli aštuonių polių 550 vatų galios LSPMSM. Daroma prielaida, kad vidinis magnetas ir vidinio magneto rotoriaus tipas leidžia pasiekti didesnį efektyvumą ir maksimalų nuolatinio srauto tankį rotoriaus paviršiuje. Pakeitus nuolatinio magneto medžiagą į NdFe35, padidėjo variklio efektyvumas ir galios tankis. Aukštose temperatūrose veikiančių galingų LSPMSM nuolatinių magnetų paviršių siūloma padengti SmCo28 medžiaga. Il. 9, bibl. 16 (anglų kalba; santraukos anglų, rusų ir lietuvių k.).